Research Article

Journal of Environmental Nanotechnology

Photosynthesis of Zinc Oxide Nanoparticles from *Portieria hornemannii:* Multifunctional Biological Activities and Molecular Docking Insights for Cervical Cancer

Abitharanitharan Kailasam Sasikala[1], M. Ponmalai[2], Rajeshkumar Shanmugam[2], Gomathy Baskar[3*] and Satheeshan Subbabhat[4]

[1]Department of Undergraduate Medical Education, Saveetha Medical College and Hospital, Saveetha Institute of Medical and Technical Sciences, Chennai, TN, India

[2]Department of Anatomy, Saveetha Medical College and Hospital, Saveetha Institute of Medical and Technical Sciences, Saveetha University, Chennai, TN, India

[3]Department of Obstetrics and Gynaecology, Saveetha Medical College and Hospital, Saveetha Institute of Medical and Technical Sciences, Saveetha University, Chennai, TN, India

[4]Department of Preclinical Sciences, Faculty of Medicine, University of West Indies, Trinidad and Tobago

Received: 10.07.2026 Accepted: 09.08.2026 Published: 30.09.2026

*gomathy3725@gmail.com

ABSTRACT

Red seaweed is regarded as an environmentally friendly and safe material for the biosynthesis of nanoparticles. Biomass of seaweeds is a renewable and commercial source of marine resources. In this research, zinc oxide nanoparticles were produced exploiting the red alga *Portieria hornemannii*. The formation of zinc oxide nanoparticles was indicated through the change in color of the test mixture recorded with the assistance of the UV-visible spectrophotometer. A variety of characterization techniques (FTIR, XRD, SEM, and EDX) were used to confirm the formation of zinc oxide nanoparticles. The effectiveness of biosynthesised zinc oxide nanoparticles was proven to be strong against Gram-positive as well as Gram-negative bacteria. The antioxidant activity of Ph-Zn-NPs was assessed using the DPPH assay, and their free radical-scavenging ability was investigated. Additionally, these nanoparticles show important anticancer activity against human cervical carcinoma (SiHa cell line) with an IC50 of 391.31±15.9. The molecular docking analysis of *P. hornemannii* compounds showed favorable binding scores with the mutated genes related to cervical cancer. The study proposes an eco-friendly and sustainable approach with a wide range of applications, particularly against cervical cancer.

Keywords: *Portieria hornemannii*; Zinc oxide nanoparticles; Antimicrobial; Anticancer; Cervical cancer; SiHa cells.

1. INTRODUCTION

Cervical cancer is a leading cause of cancer-related deaths among women worldwide, particularly in developing countries where screening and treatment options are limited. High-risk human papillomavirus (HPV) strains are central to cervical carcinogenesis, leading to genomic instability and tumor progression (Anupama *et al.* 2026). Conventional treatments like chemotherapy and radiotherapy often yield severe side effects and drug resistance, underscoring the need for alternative, safer anticancer agents. Nanotechnology offers a promising avenue for cancer therapeutics due to the unique properties of nanoparticles, which facilitate targeted delivery, enhanced cellular uptake, and induction of apoptosis in cancer cells (Aruchamy *et al.* 2026). Zinc-based nanoparticles, through reactive oxygen species (ROS) generation and other mechanisms, demonstrate strong anticancer potential, especially when integrated with bioactive metabolites from marine sources like *P. hornemannii*.

Nanoscience is the scientific study of substances that have at least one dimension in the 1–100 nm range. It involves the arrangement of atoms/molecules into nanoparticles/ nano-materials or the destruction of a macroscopic substance. Recently, the field of nanomaterial production technology has gained importance due to the potential of nanomaterials in numerous fields (Abdullah *et al.* 2020). During the past few decades, the number of scientific fields, industrial areas, as well as devices employing nanotech has dramatically increased (Zangeneh *et al.* 2020). In green synthesis, there are some benefits, such as an easy, fast preparation process and low cost and waste generation (Kiwumulo *et al.* 2022; Sahith *et al.* 2026). Zinc oxide nanoparticles (ZnO-NPs) are particularly notable for their optical, chemical, and biological characteristics, including biocompatibility, controlled drug release capabilities, and inherent antimicrobial and anticancer effects. These properties enhance cellular uptake and enable selective toxicity towards cancer cells, making

ZnO-NPs promising for oncological treatments. Traditional synthesis methods for metal nanoparticles often entail high energy consumption and hazardous by-products; in contrast, Biological synthesis using plant-derived extracts provides an eco-friendly and sustainable approach for nanoparticle fabrication, as plant biomolecules can facilitate the reduction and stabilization of metal nanoparticles (Rahman *et al.* 2026; Sivaranjani and Parthiban, 2025).

Marine macroalgae are increasingly valued for their bioactive metabolites, which serve as natural reducing, stabilizing, and capping agents in nanoparticle synthesis. These biomolecule-mediated nanoparticles often demonstrate enhanced stability and reduced toxicity (Doan *et al.* 2026). For example, *Portieria hornemannii* is recognized for its rich array of bioactive compounds, including phenolics, flavonoids, terpenoids, and sulfated polysaccharides, contributing to its antioxidant, antimicrobial, anti-inflammatory, and anticancer properties. Due to variations in phytochemical composition influenced by environmental factors, standardized extraction and characterization methods are crucial for reproducibility in nanoparticle synthesis. While research on marine-derived nanoparticles is expanding, studies specifically utilizing *P. hornemannii* for synthesizing ZnO-NPs remain limited. The seaweed's bioactive constituents have the potential to enhance nanoparticle stability and biological function, making it a promising candidate for nanotechnology applications in therapeutics (Baskar *et al.* 2025).

The antioxidants present in natural compounds, especially from marine origin, such as *P. hornemannii*, are gaining attention for their role in neutralizing ROS and preventing cellular damage (Shobier *et al.* 2026). The combination of metal oxides with plant metabolites in green-synthesized nanoparticles could enhance antioxidant capabilities, paving the way for potent antioxidant therapies. Furthermore, as multidrug-resistant (MDR) microorganisms rise, there is a pressing need for effective antimicrobial agents. Zinc nanoparticles possess antibacterial and antifungal properties, and the bioactive metabolites from *P. hornemannii* can improve their stability and efficacy, presenting a sustainable strategy for combating pathogens in various sectors, including biomedical and environmental applications (Kalaba *et al.* 2024). Even though there has been growing interest in the synthesis of nanoparticles by seaweed, the use of *Portieria hornemannii* for the environment-friendly fabrication of ZnO-NPs and the assessment of their effectiveness and biological activities related to their stability behavior have not been thoroughly investigated. The significance of the research is that the possibility of using the extract of *P. hornemannii*, rich in phytochemicals, as a reducing and stabilizing agent for the production of non-toxic ZnO-NPs has been developed.

2. MATERIALS AND METHODS

2.1 Reagents Used

Zinc acetate, Ascorbic acid, Diphenyl picrylhydrazyl (DPPH), Mueller-Hinton agar, Nutrient Broth, Dulbecco's modified Eagle medium (DMEM), fetal bovine serum (FBS), 100X phosphate-buffered saline (PBS), trypsin-EDTA, and antibiotic and antimycotic solution were bought from Gibco, Thermo Scientific, India. Ascorbic acid and Methyl thiazole tetrazolium (MTT) salt were bought from HiMedia, India.

2.2 Seaweed Sample Collection

Red seaweed *Portieria hornemannii* was collected from the seashore of Mandapam (Lat. 09°17′ N; Long. 79°08′ E) of Ramanathapuram district, Tamil Nadu, India. The algal sample was taxonomically identified by the Central National Herbarium, Howrah, India (CHN/Tech.II/2022/8). The washed seaweed collected from the sea was washed thoroughly in tap water to remove adhered material/impurities and in distilled water to remove any adsorbed pollutants, and then the shade-dried algal biomass was finely powdered.

2.3 Synthesis of Zinc Oxide Nanoparticles

Zinc oxide nanoparticle synthesis through biological processes: 1 gram of *P. hornemannii* samples and one hundred millilitres of distilled water were heated in an Erlenmeyer flask at 45°C for fifteen minutes while being stirred with a hot plate magnetic stirrer. Following this, when the extract had cooled down to room temperature, it was passed through filter paper (Whatman No.1) to separate any suspended or solid matter/impurity, leaving a solution called the filtrate. This filtrate was then used as an essential part of the zinc nanoparticle production process. A 1 mM zinc acetate solution (95 mL) was mixed with *P. hornemannii* extract (5 mL) to initiate the formation of Zn-NPs. The reaction mixture was stirred using a magnetic stirrer for 3- 4 h at 70°C until a color change occurred. The solution of Zn-NPs was centrifuged at 4,000 rpm for 10 minutes. As a result of centrifugation, Zn-NPs settled at the bottom of the tube. After that, they were taken from the liquid, washed, and dried to be used for further studies (Ishwarya *et al.* 2018).

2.4 Characteristics of a Zinc Oxide Nanoparticle

Techniques for characterising the optical properties of the produced zinc oxide nanoparticles were evaluated using UV-Vis spectroscopy equipment (Shimadzu Corporation, Japan). In this work, we used a restricted wavelength range (350 nm to 800 nm) to identify the maximum absorption peak of synthesized Zn-NPs. To more precisely describe different-sized nanoparticles, the crystalline phase of the zinc oxide nanoparticles was identified using X-ray diffraction (PANalytical, Netherlands) analysis. Fourier transform infrared spectroscopy, or FTIR, is an efficient analytical technique (Shimadzu, Irtracer 100) employed in the research of nanoparticles to investigate their chemical makeup. For this investigation, scan speeds ranging from

400 to 4000 cm^{-1} were employed. These measurements were obtained at a rate of 32 scans per minute and have a resolution of 1- 4 cm^{-1}.

2.5 Antimicrobial Activity

The microorganisms utilized in this research work included *Staphylococcus aureus*, *Pseudomonas aeruginosa*, *Klebsiella pneumoniae*, and *Escherichia coli*, which were procured from the Microbial Type Culture Collection (MTCC), India. These microbial strains were cultured and preserved in Nutrient broth. The antibacterial effect of *P. hornemannii*-ZnO-NPs against bacterial strains was assessed by means of agar well diffusion. Bacteria that had grown for 24 hours were used to inoculate Mueller-Hinton agar plates. The agar wells, each being 6 mm in diameter, were punched out. The control antibiotic (Penicillin/Streptomycin) (30 µL), along with biosynthesised zinc oxide nanoparticles (25, 50 and 100 µL each), was added inside each of the wells. Following that, the plates were incubated at 37°C for 24 hours.

2.6 Antioxidant Activity

A solution of DPPH in ethanol with a concentration of 0.1 mM was prepared to examine its radical scavenging potential. Subsequently, biosynthesized zinc nanoparticles were introduced at varying amounts of 10, 20, 30, 40, and 50 µg/mL. The absorbance was measured at a wavelength of 517 nm using a UV-visible spectrophotometer. The calculated percentage of inhibition was determined through the equation as follows:

$$\text{Percentage of inhibition} = [(Ab - As) / Ab] \times 100$$

Ab is the absorbance of the blank and As is the absorbance of the ZnO-NPs.

2.7 Anti-inflammatory Activity

Bovine serum albumin (BSA) (0.45 mL) was combined with various concentrations of Zn-NPs (10–50 g/mL) of *P. hornemannii*. The pH level was then adjusted to 6.3. The mixture was kept at room temperature for 10 minutes and then incubated in a water bath at 55°C for 30 minutes. The reference was diclofenac sodium, and the control was DMSO. The samples were tested using a spectrophotometer at 660 nm. The percentage of protein denaturation was calculated as follows:

$$\text{Percentage of Inhibition} = [(Ab-As) / Ab] \times 100$$

Ab represents the absorbance of the blank, and As stands for the absorbance of the Zn-NPs.

2.8 Anticancer Activity

2.8.1 Cancer Cell Line Maintenance

The cell lines utilized in this study encompassed the SiHa cervical cancer cell line. Human cervical cancer cell lines were sourced from the National Centre for Cell Sciences (NCCS) based in Pune, India. Cell proliferation was maintained in Dulbecco's Modified Eagle's Medium (DMEM) together with 10 % foetal bovine serum (FBS) and 1% anti-mitotic agent. The culture was performed in this medium. The culture was kept in a humidified chamber with 5 % CO_2 and a temperature of 37 ◦C. Cell lines grown in T-25 tissue culture flasks were counted.

2.8.2 In Vitro Cytotoxicity Activity of Synthesized *P. hornemannii*-ZnO-NPs

The cytotoxicity of cells was investigated in vitro by means of the MTT Assay (3-(4,5-dimethylthiazol-2-yl)-2,5-diphenyltetrazolium bromide). After the cells were plated on a 96-well plate (1 × 10 ^5 cells/well), they were treated with various concentrations of ZnO-NPs (1 mg/mL) in complete medium for 24 h (50- 500 µg/mL). The cells that were not treated with ZnO-NPs served as a control. The wells with the treated and untreated cells were given 50 µl of MTT solution with a concentration of 5 mg/mL for the assay. After 4 h of incubation of MTT-treated cells at 37◦C, DMSO was added in place of the culture medium. Light absorption readings were taken at 630 nm using the ELISA plate reader (LabServ-ELISA Plate Reader) (Baskar *et al.* 2024).

2.9 In Silico Molecular Docking Analysis

Molecular docking is a very useful tool within structural biology and drug development fields, since it predicts how different ligands and proteins interact with one another. It also helps determine preferred orientations and binding affinities. P_yR_x was used to perform virtual docking simulations, while Discovery Studio was employed to analyse the results of the simulated interactions.

2.9.1 Ligand File Preparation

According to Arumugam *et al.* (2022), a GC/MS analysis of the *Portieria hornemannii* fraction led to a series of bioactive substances being identified in the seaweed. Molecular interaction studies between the compounds identified in the seaweed and the proteins responsible for triple-negative breast cancer were carried out using the P_yR_x software. The database containing information regarding the various ligands refers to the identification information of the chemical compounds lying in the PubChem database. The ligands associated with the identification are n-hexadecanoic acid (Pubmed ID: 985) and 9,12-Octadecadienoic acid (PubMed ID: 5280450) and hexadecanoic acid, 2-Hydroxyethyl ester (PubMed ID: 123409) and 9-octadecadienoic acid-hydroxy methyl (Pubmed ID: 5319879) and oleic acid (Pubmed ID: 445639) and Paclitaxel (Pubmed ID: 36314) respectively. All the ligands were then converted from SDF to PDB format using the PyMOL software. The AutoDock P_yR_x tools were employed for docking the

ligands. Molecular docking and binding affinity assessments were performed through the P_yR_x software using a command-line interface. The P_yR_x system settings for the ligand and receptor were provided with the respective names of the ligand and target protein using a pdbqt extension. The settings establish the size and the center of the grid. The proteins are distinct from each other and may exist in different forms. The docking results are converted to a text log file and a pdbqt file. The grid specifications included information about sizes and centers in x, y, and z directions.

2.9.2 Protein File Preparation

The proteins under evaluation for docking simulations and their importance in the process of cervical cancer identification. The 3D models of proteins were sourced from the RCSB database in the PDB format. The selected proteins include: PIK3CA (PDB ID: P42336), PTEN (PDB ID: P60484), RICTOR (PDB ID: Q6R327), STK11 (PDB ID: Q15831), and AKT2 (PDB ID: P31751). In order to obtain the proteins' 3D structures, any ligands and water molecules present in the original models were eliminated. The structures were processed by creating hydrogen bonds and recording them in the pdb file for future docking studies.

2.9.3 Active Site Prediction

The CASTp server was used in the study to find active sites of the proteins of concern. After importing the PDB file, one could easily determine the active sites by inputting the relevant coordinates on the website. The residues corresponding to the active sites were then used to calculate the size of the grid box in PyRx Tools for the docking process.

2.10 Statistical Analysis Data

The reported results included standard deviations along with the mean values. Microsoft Excel 2019 was used to analyze the control and test values. The results are deemed significant if $p < 0.05$.

3. RESULTS AND DISCUSSION

3.1 Zinc Oxide Nanoparticle Synthesis

The process of ZnO NPs formation was tracked through visual assessment. The color changed from white to pale yellow, indicating ZnO NPs formation through the *P. hornemanini* process. Seaweed metabolites reduced the metal precursor to nanostructures, as shown by the progressive color shift. The stimulation of plasmon vibrations on the surface of metal and metal oxide NPs is responsible for the highest color change seen in the current investigation after 24 hours.

3.2 Characterization of Zinc Oxide Nanoparticles

3.2.1 UV-visible Spectroscopy

The UV–Visible spectrum confirmed the formation of ZnO nanoparticles. At 0 h, the reaction mixture showed very low absorbance, indicating that nanoparticle formation had not yet occurred. Using UV-Vis spectroscopy, the highest absorbance corresponding to the maximum SPR of ZnO-NPs was detected. The SPR peaks were obtained in the UV region due to oscillations of electrons in the conduction band under the influence of an electromagnetic field (Marica *et al.* 2022). The maximum intensity and width of peaks depend on the size, shape, and temperature of nanoparticles (Fouda *et al.* 2023). In this research, the maximum SPR of phyto-fabricated ZnO-NPs was found at 360 nm (Fig. 1). The peak of absorption appeared in the range of light absorption of ZnO-NPs in the band of 350–380 nm.

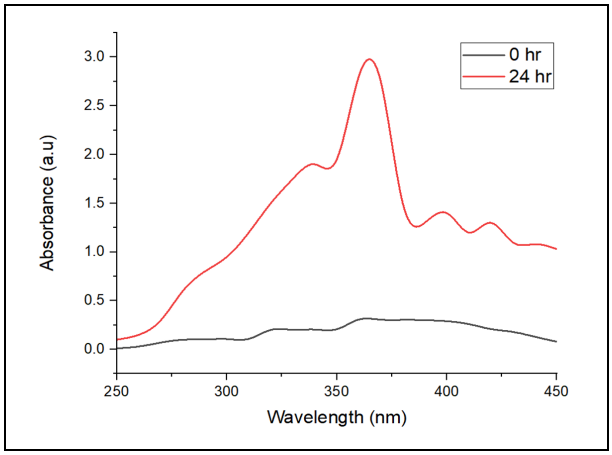

Fig. 1: UV-visible spectroscopy analysis of *P. hornemannii*-ZnO-NPs

In addition to capping with Zn^{2+} ions and causing the nucleation of ZnO, these components have other chelating and reducing characteristics. While phenolic chemicals create multi-chelating bonds and stabilize the ZnO-NPs following nucleation, flavonoid moieties start the capping on Zn^{2+} ions, resulting in the creation of various-sized nanoparticles (Abomuti *et al.* 2021). A blue shift, which is seen when particle size decreases, causes the peak to move to a lower wavelength (Mohammadian *et al.* 2018). In addition to demonstrating the creation of zinc oxide nanoparticles using the green synthesis process, the absorption peaks also demonstrate the simultaneous vibration of the nanoparticles' electrons and light waves. The recorded maximum values are within the wavelength range of 360-380 nm for the light absorption spectrum of ZnO nanoparticles (Ifeanyichukwu *et al.* 2020). Ezealisiji *et al.* (2019) gave similar findings, and Rajeshkumar *et al.* (2018) fabricated ZnO nanoparticles using Magnifera indica and obtained a measurable peak at a wavelength of 355 nm.

3.2.2 FTIR Analysis

The FTIR spectrum was used to identify the functional groups involved in the synthesis of ZnO nanoparticles. A broad peak at 3389 cm^{-1} corresponds to the O–H stretching vibration of hydroxyl groups present in phenolic compounds and alcohols. The absorption band at 2941 cm^{-1} is attributed to the C–H stretching vibration of aliphatic groups. The peak observed at 1611 cm^{-1} is assigned to C=O stretching of amide groups or C=C stretching of aromatic compounds. The bands at 1407, 1227, 1151, 1077, and 1018 cm^{-1} indicate the presence of C–O, C–N, and C–O–C functional groups associated with proteins, polysaccharides, and polyphenols. The peaks at 986, 833, 766, and 729 cm^{-1} are related to C–H bending vibrations of aromatic compounds (Fig. 2). These results suggest that the phytochemicals present in the seaweed extract played an important role in reducing zinc ions and stabilizing the synthesized nanoparticles. The reduction of Zn^{2+} may have been facilitated by the presence of functional groups such as amines, alcohols, ketones, phenols, carboxylic acids, and alkenes in the seaweed extract of *Portieria hornemannii*. The presence of these functional groups plays an important role in promoting cellular uptake in the process of endocytosis while promoting action against cancer cells (Augustine *et al.* 2020). These biocomponents are important in controlling the shape and size of the nanoparticle and in improving their stability, which influences their performance in biology (Ashraf *et al.* 2023).

Furthermore, the existence of free amino and carboxylic group contacts with the zinc oxide nanoparticle surface is associated with the stability of the generated zinc oxide nanoparticles, whereas the action of carboxylic and phenolic acids is responsible for bio-capping during synthesis (Hamad *et al.* 2025).

3.2.3 XRD Analysis

The crystalline nature of the biosynthesized ZnO nanoparticles was investigated using X-ray diffraction (XRD). The diffraction pattern exhibited characteristic peaks at approximately 31.8°, 34.4°, and 36.3°, corresponding to the (100), (002), and (101) crystal planes, respectively (Fig. 3). These diffraction planes are characteristic of the hexagonal wurtzite structure (JCPDS No. 36–1451) of ZnO, confirming the successful formation of ZnO nanoparticles (Mongy *et al.* 2024). In contrast, the diffractogram exhibited background peaks at 2θ, which are often seen in green synthesis techniques and can be associated with the crystallization of organic components deriving from the fruit extract onto the surface of NPs (Islam *et al.* 2025).

The broad and relatively low-intensity peaks indicate that the nanoparticles are nanosized and possess low crystallinity, which is commonly observed in green-synthesized nanoparticles due to the presence of phytochemical capping agents. The absence of additional diffraction peaks suggests that no detectable crystalline impurities were present in the synthesized sample. The XRD spectra of zinc oxide nanoparticles made with *Portieria hornemannii* seaweed show no additional peaks, indicating that the synthesized nanoparticles are pure, which affirms the applicability of this green synthesis method for the production of highly pure nanoparticles (Akbarian *et al.* 2018).

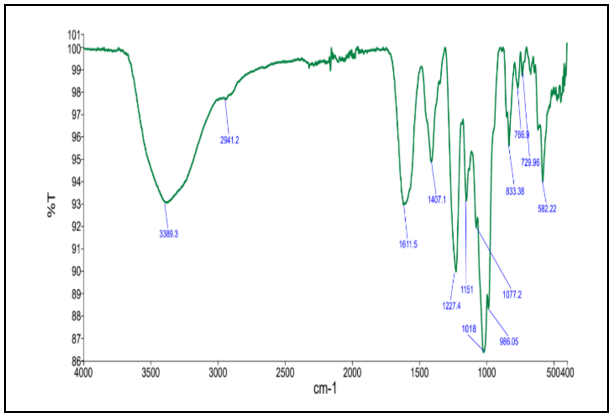

Fig. 2: FTIR analysis of *P. hornemannii*-ZnO-NPs

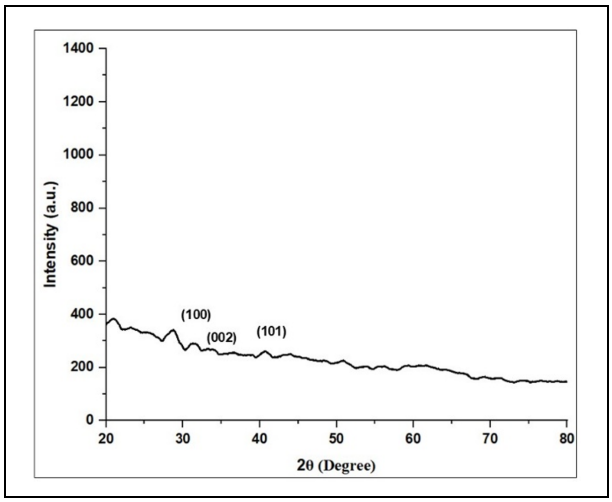

Fig. 3: XRD analysis of *P. hornemannii*-ZnO-NPs

3.2.4 SEM Analysis

The surface morphology of the biosynthesized ZnO nanoparticles was examined using scanning electron microscopy (SEM). The SEM pictures indicated that the nanoparticles were irregularly shaped and highly aggregated, producing compact clusters, comparable to the findings of Umar *et al.* (2019) and Muhammad *et al.* (2019), and the presence of agglomerated nanoparticles can be seen on the SEM image (Fig. 4). The aggregation of nanoparticles may be attributed to their high surface energy and the interaction of phytochemicals present in the seaweed extract, which act as natural capping agents.

This indicates that the synthesized nanoparticles are in their purest form.

3.2.5 EDX Analysis

The elemental composition of the biosynthesized ZnO nanoparticles was confirmed by EDX analysis. The spectrum showed prominent peaks corresponding to zinc (Zn) and oxygen (O), confirming the successful formation of ZnO nanoparticles. Furthermore, carbon peaks were found that corresponded to biological compounds such as vitamins, polyphenols, flavonoids, amino acids, and saponins (Fig. 5). At around 1 keV, 1.3 keV, and 2.3 keV, zinc showed three separate peaks, whereas oxygen showed a single peak at about 0.5 keV (Islam *et al.* 2025). These peaks are consistent with the characteristic signatures of ZnO NP. These elements are likely derived from the phytochemicals and mineral constituents naturally present in the seaweed extract, which act as reducing and stabilizing agents during nanoparticle synthesis. The absence of impurity peaks from other metals indicates the high purity of the synthesized ZnO nanoparticles. Overall, the EDX results support the successful green synthesis of ZnO nanoparticles.

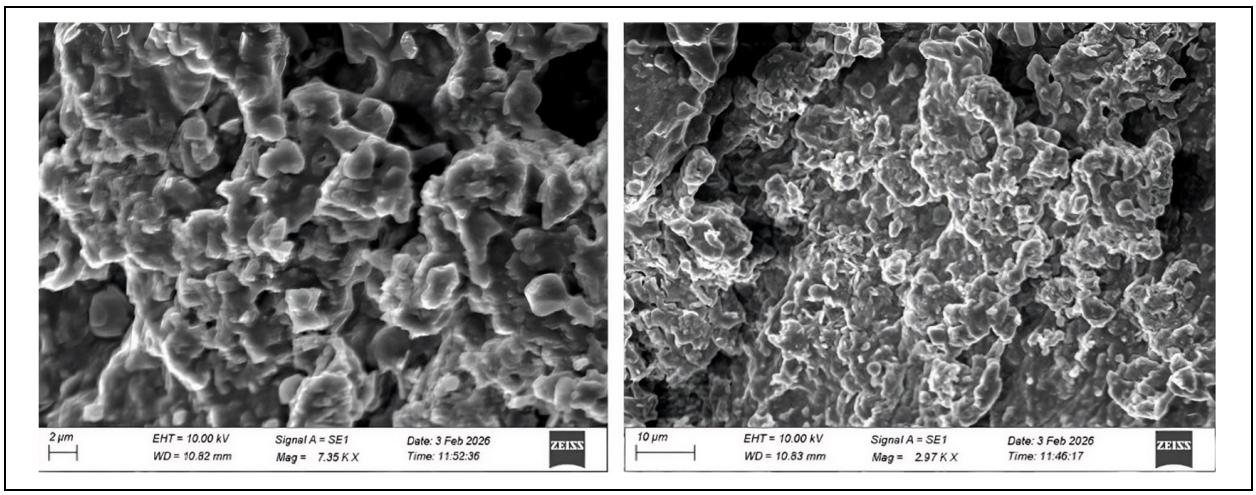

Fig. 4: SEM analysis of *P. hornemannii*-ZnO-NPs

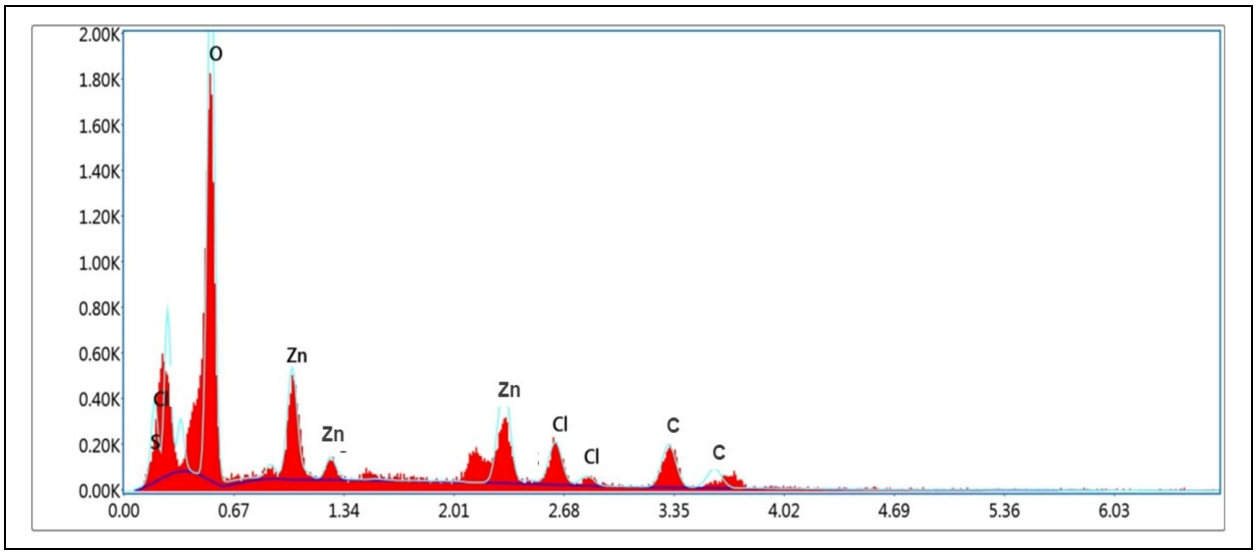

Fig. 5: EDX analysis of *P. hornemannii*-ZnO-NPs

3.3 Antimicrobial Activity

The agar well diffusion method was employed to test the antibacterial efficacy of the biosynthesized zinc oxide (ZnO) nanoparticles using *P. hornemannii* on both Gram-negative and Gram-positive bacteria. The zinc nanoparticles developed using *P. hornemannii* exhibited good antibacterial activity against all tested bacteria, including *E. coli*, *P. aeruginosa*, *S. aureus*, and *K. pneumoniae*, at concentrations of 25, 50, and 100 µg/µL. The maximum zone of inhibition observed with ZnO NPs treatment is 100 µg/mL against *K. pneumoniae* and *P. aeruginosa*. The effect of ZnO NPs on *E. coli* is average (Fig. 6&7). The data reported here show that

antimicrobial activity increases as the dosage increases, and the ZnO NPs synthesized have shown commendable antibacterial effects. The strong antibacterial effect of ZOI of ZnO NPs can be interpreted as a synergistic effect of a harmless antimicrobial composite. According to Pillai *et al.* (2020), the antibacterial effect of the green-synthesized ZnO increases proportionately to the concentration of NPs.

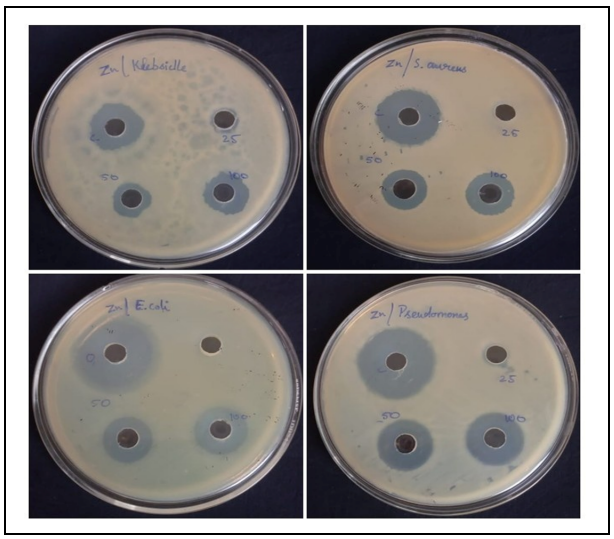

Fig. 6: Zone of inhibition of Ph-ZnO-NPs

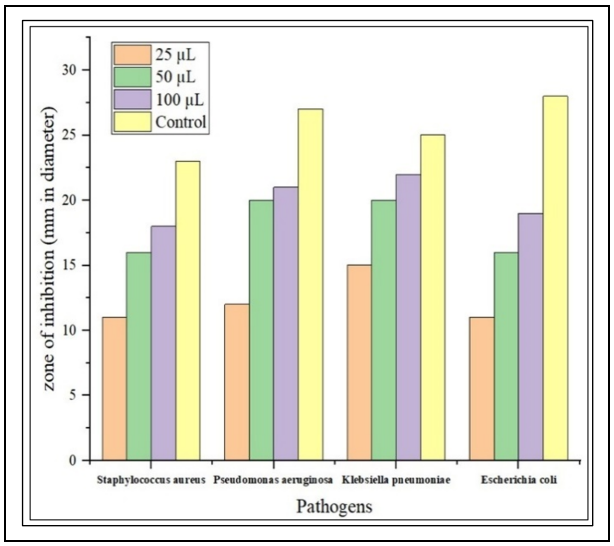

Fig. 7: Antimicrobial activity of Ph-ZnO-NPs

3.4 Antioxidant Activity

Free radical molecules that have unpaired electrons are produced during cellular metabolism, and they are known to be very reactive and able to damage cells. Seaweeds and their constituents are regarded as powerful antioxidants. Antioxidants are stable compounds that donate electrons to neutralize free radicals and lessen oxidative stress. Polyphenolic compounds that are classified as secondary metabolites found in seaweeds are responsible for regulating antioxidant levels in animals (Palanisamy *et al.* 2017). The study's authors showed that Ph-ZnO-NPs had a concentration-dependent capacity for scavenging DPPH radical, with maximum inhibition of 55.8% at the concentration of 50 µg/mL (Fig. 8). Meanwhile, the control ascorbic acid produced inhibition of 78.5% at the highest dose used in the experiments. The interaction between biosynthesized nanoparticles and DPPH radical was demonstrated, which leads one to assume that this effect can be explained by the article authors and results of earlier studies about the electron transfer occurring at the oxygen sites located on the radicals (Mirza *et al.* 2018).

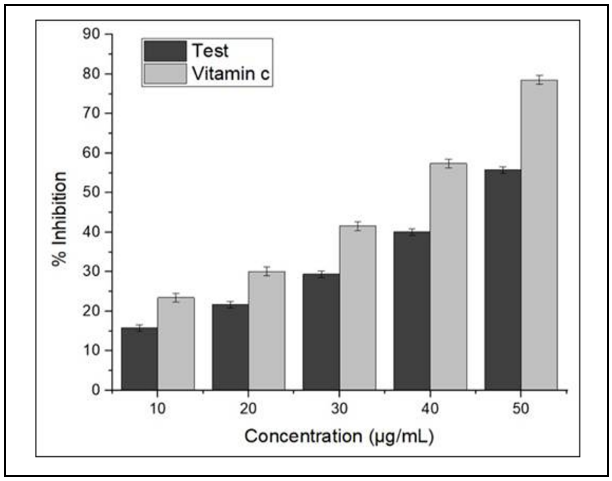

Fig. 8: Antioxidant activity of Ph-ZnO-NPs

3.5 Anti-inflammatory Activity

The anti-inflammatory activity of the biosynthesized ZnO nanoparticles was evaluated using the protein denaturation assay and compared with the standard drug, diclofenac sodium. As shown in Fig 9, the nanoparticles exhibited a concentration-dependent increase in anti-inflammatory activity. The percentage inhibition increased from 20% at 10 µg/mL to 64% at 50 µg/mL, indicating that higher concentrations enhanced the inhibition of protein denaturation. In comparison, diclofenac sodium showed greater activity, with inhibition values ranging from 43% to 86% over the same concentration range. Although the standard drug demonstrated higher efficacy, the biosynthesized ZnO nanoparticles exhibited appreciable anti-inflammatory activity. This effect may be attributed to the bioactive compounds from the seaweed extract present on the nanoparticle surface, which can stabilize proteins and reduce inflammatory responses (Gunasekaran *et al.* 2026). *Anoectochilus elatus*-ZnONPs demonstrated a maximum inhibition of 76.02%, whereas conventional aspirin showed a maximum inhibition of 86% at 50 µg/mL (Vijayakumar *et al.* 2022). These findings suggest that the green-synthesized ZnO nanoparticles possess promising anti-inflammatory properties and may serve as

a potential natural alternative for managing inflammatory conditions.

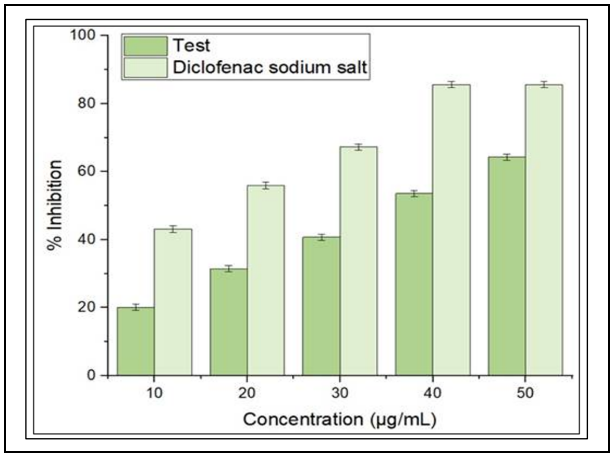

Fig. 9: Anti-inflammatory activity of Ph-ZnO-NPs

3.6 Anticancer Activity

The cytotoxic effect of the biosynthesized ZnO nanoparticles (Ph-Zn) was evaluated against cancer cells using the MTT assay. As shown in Fig. 10, cell viability decreased in a concentration-dependent manner following treatment with Ph-Zn nanoparticles. The percentage of viable cells decreased from 95% at 50 µg/mL to 22% at 500 µg/mL, indicating a significant increase in cytotoxicity with increasing nanoparticle concentration. The IC_{50} value was determined to be 391.31 ± 15.9 µg/mL, demonstrating the ability of the nanoparticles to inhibit cancer cell growth. Microscopic examination further supported the MTT results. Untreated control cells (Fig. 10A) exhibited normal morphology with intact cell membranes and good adherence. In contrast, cells treated with Ph-ZnO nanoparticles (Fig. 10B) showed noticeable morphological changes, including cell shrinkage, rounding, loss of adhesion, and a reduced number of viable cells. These observations indicate nanoparticle-induced cellular damage and cell death. Zinc in cancer cells is vital to the development and progression of cancer. High levels of Zinc may be toxic, while low levels have been related to a wide variety of cancers (Sugimoto *et al.* 2024).

Overall, the findings show that biosynthesized ZnO nanoparticles have concentration-dependent anticancer action and significantly reduce cancer cell survival, indicating their potential as a promising alternative for future anticancer research. Zinc oxide nanoparticles' anticancer effects might be attributed to the formation of reactive oxygen species capable of controlling mitochondrial enzymes. Furthermore, these nanoparticles may activate numerous additional pathways, such as DNA damage, membrane breakdown, cell death, and cell cycle arrest, all adding to their potential to kill cancer cells (Yusefi *et al.* 2020). According to other researchers, ZnO-NPs are exclusively harmful to malignant cell types and have no cytotoxic impact on healthy cells (El-Belely *et al.* 2021).

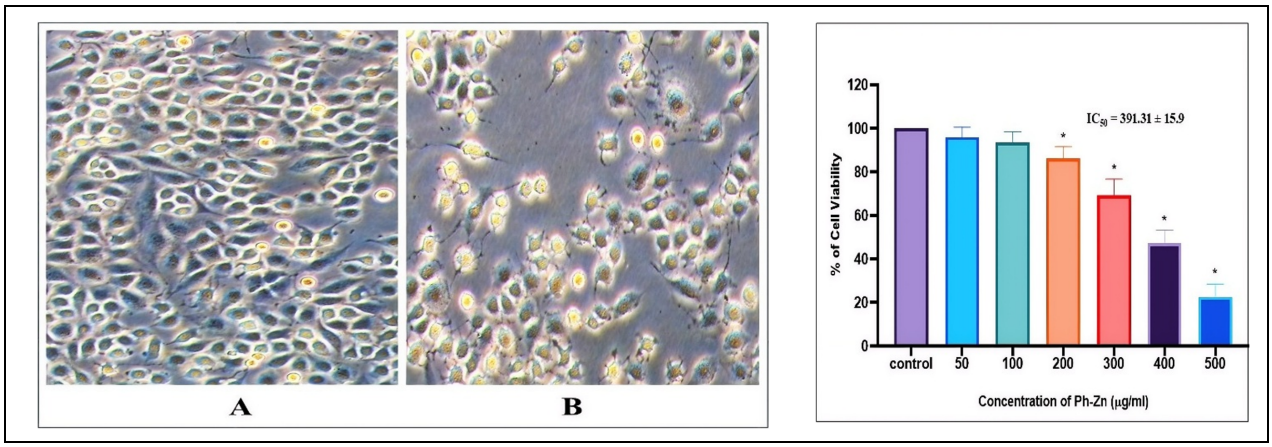

Fig. 10: Anticancer activity of Ph-ZnO-NPs

3.7 Molecular Docking

An investigation of molecular docking was carried out in order to find possible lead medication candidates for the treatment of cervical cancer. A docking method was developed using P_yR_x software to align ligands with the receptor protein's binding pocket, which contains the active amino acids. To visualize the docked configurations, Discovery Studio Visualizer was used, allowing for the examination of 3D Structures that demonstrated the interactions of amino acids, proteins, and compounds. The standard drug paclitaxel was used as a reference to compare molecular docking scores for selected drugs in *P. hornemannii*.

The docking analysis showed higher binding affinity against the oleic acid compound for the PTEN protein (-5.7), and 9, 12-octadecadienoic acid (Z, Z) showed a higher binding affinity for PIK3CA (-5.5), STK11 (-5.3) and AKT2 (-5.4) proteins. 9-Octadecenoic

acid (Z), 2-hydroxy-1(hydroxymethyl)ethyl shows a higher binding affinity for RICTOR protein (-5.3). Paclitaxel, a drug compound, showed better binding affinity for AKT2 protein. This bioinformatic analysis proved that 9, 12-octadecadienoic acid (Z, Z) showed effective binding affinity against highly mutated genes in cervical cancer (Fig. 11) (Table 1). Consequently, ZnO-PS NPs induce mitochondrial depolarization and cause cell death by apoptosis by promoting apoptotic genes and blocking anti-apoptotic genes (Rizvi *et al.* 2026).

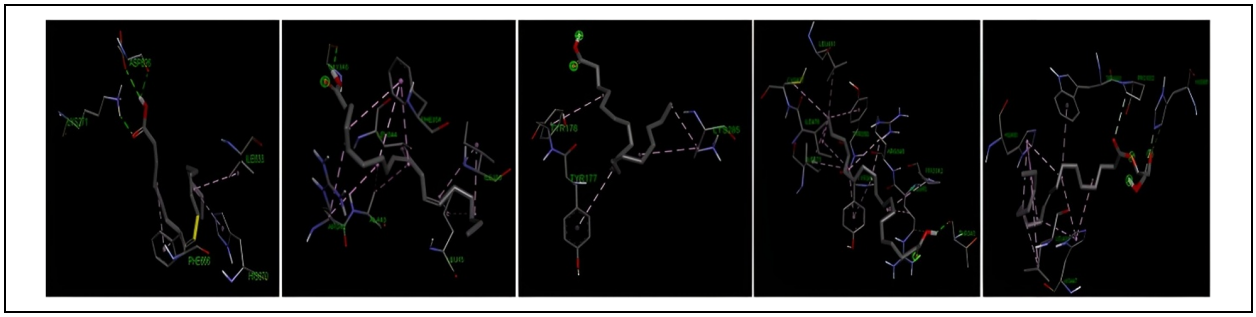

Fig. 11: Molecular interaction of *P. hornemannii* compounds and cervical cancer proteins

Table 1. Molecular docking analysis and its interaction score

Molecular Docking Interaction Score (kcal/mol)					
Ligands (Seaweed Compounds)	Proteins in Cervical Cancer				
	PIK3CA	PTEN	RICTOR	STK11	AKT2
n-hexadecanoic acid	-5.1	-4.8	-4.5	-4.4	-4.7
9, 12-octadecadienoic acid (Z, Z)	-5.5*	-5.5	-5.1	-5.3*	-5.4*
Hexadecanoic acid, 2-hydroxy-1-(hydroxymethyl)ethyl ester	-4.8	-4.7	-4.9	-4.9	-5.2
9-Octadecenoic acid (Z), 2-hydroxy-1(hydroxymethyl)ethyl	-5.2	-5.5	-5.3*	-4.9	-5.2
Oleic acid	-5	-5.7*	4.7	-5.1	-5.2
Paclitaxel	-9.7	-8.1	-8.9	-7.2	-9.9

***- Highest Binding affinity**

4. CONCLUSIONS

This study successfully demonstrated the green synthesis of zinc oxide nanoparticles from *P. hornemannii* extract, which acted as a natural reducing and stabilising agent. The visual color change and UV-Vis spectra confirmed nanoparticle formation, and FTIR analysis identified the functional biomolecules that were responsible for capping. XRD analysis revealed that the zinc oxide nanoparticles have a crystalline nature. The morphology and elemental composition of the Ph-ZnO-NPs were validated using SEM and EDX analysis. Ph-ZnO-NPs were shown to have antibacterial properties against both Gram-positive and Gram-negative bacteria. ZnO-NPs showed strong antioxidant activity that was comparable to that of ascorbic acid, indicating that they might be useful antioxidants. Additionally, these nanoparticles demonstrated encouraging anticancer activities against human cervical cancer (SiHa) cells, resulting in decreased cell viability and cell death. Molecular docking analysis conducted on compounds originating from seaweed was found to have positive binding results against the proteins related to cervical cancer mutations, with 9, 12-octadecadienoic acid being particularly active against many target proteins. Thus, bioactive compounds and Ph-ZnO-NPs indicate more possibilities for therapeutic application, reinforcing the idea of developing novel drugs for curing cervical cancer. Overall, using *P. hornemannii* Zn-NPs makes them stable, nanoscale in size and very pure. The use of *P. hornemannii* offers an eco-friendly, cost-effective, safe and sustainable approach for nanoparticle synthesis, with potential applications in the biomedical field.

FUNDING

This research received no specific grant from any funding agency in the public, commercial, or not-for-profit sectors.

CONFLICTS OF INTEREST

The authors declare that there is no conflict of interest.

COPYRIGHT

This article is an open-access article distributed under the terms and conditions of the Creative Commons Attribution (CC BY) license (http://creativecommons.org/licenses/by/4.0/).

REFERENCES

Abdullah, J. A. A., Eddine, L. S., Abderrhmane, B., Alonso-González, M., Guerrero, A. and Romero, A., Green synthesis and characterization of iron oxide nanoparticles by *Phoenix dactylifera* leaf extract and evaluation of their antioxidant activity, *Sustain. Chem. Pharm.*, 17, 100280 (2020). https://doi.org/10.1016/j.scp.2020.100280

Abomuti, M. A., Danish, E. Y., Firoz, A., Hasan, N. and Malik, M. A., Green synthesis of zinc oxide nanoparticles using *Salvia officinalis* leaf extract and their photocatalytic and antifungal activities, *Bio.*, 10(11), 1075 (2021). https://doi.org/10.3390/biology10111075

Akbarian, M., Mahjoub, S., Elahi, S. M., Zabihi, E. and Tashakkorian, H., *Urtica dioica* L. extracts as a green catalyst for the biosynthesis of zinc oxide nanoparticles: characterization and cytotoxic effects on fibroblast and MCF-7 cell lines, *New J. Chem.*, 42(8), 5822–5833 (2018). https://doi.org/10.1039/c8nj00496j

Anupama, C. V., Devarapalli, D., Ahammad, S. H., Eid, M. and Rashed, A. N. Z., Cervical cancer cell prediction and detection with high test accuracy based on a reliable automated system, *3 Biotech*, 16(2), 83 (2026). https://doi.org/10.1007/s13205-026-04702-5

Aruchamy, M., Ramanathan, S., Shanmugam, N. and Muthupandian, S., Deciphering autophagy-metabolism interactions in cancer drug resistance: a comprehensive review, *Cancer Chemother. Pharmacol.*, 96(1), 38 (2026). https://doi.org/10.1007/s00280-026-04894-w

Arumugam, M., Karuppannan, S., Govindasamy, B., Palaniappan, N., Lakshmanan, A. and Maluventhan, V., Radicals scavenging potentials and mosquito vectors' biocontrol measures from bioactive principles of the marine red algae *Portieria hornemannii*, (2022). https://doi.org/10.21203/rs.3.rs-1553020/v1

Ashraf, H., Meer, B., Iqbal, J., Ali, J. S., Andleeb, A., Butt, H., Zia, M., Mehmood, A., Nadeem, M., Drouet, S. and Blondeau, J. P., Comparative evaluation of chemically and green synthesized zinc oxide nanoparticles: their in vitro antioxidant, antimicrobial, cytotoxic and anticancer potential towards HepG2 cell line, *J. Nanostruct. Chem.*, 13(2), 243-261 (2023). https://doi.org/10.1007/s40097-021-00460-3

Augustine, R., Hasan, A., Primavera, R., Wilson, R. J., Thakor, A. S. and Kevadiya, B. D., Cellular uptake and retention of nanoparticles: Insights on particle properties and interaction with cellular components, *Mater. Today Commun.*, 25, 101692 (2020). https://doi.org/10.1016/j.mtcomm.2020.101692

Baskar, G., Palaniyandi, T., Al-Mutiry, M., Alshammari, N. and Saeed, M., Biocatalytic green synthesis of iron oxide nanoparticles using red seaweed *Portieria hornemannii* for biomedical applications, *Biocatal. Agric. Biotechnol.*, 70, 103831 (2025). https://doi.org/10.1016/j.bcab.2025.103831

Baskar, G., Palaniyandi, T., Ravi, M., Viswanathan, S., Wahab, M. R. A., Surendran, H., Govindaraj, M., Sugumaran, A., Almutairi, M. H. and Almutairi, B. O., Biosynthesis of iron oxide nanoparticles from red seaweed Hypnea valentiae and evaluation of their antioxidant and antitumor potential via the AKT/PI3K pathway, *Process Biochem.*, 141, 155-169 (2024). https://doi.org/10.1016/j.procbio.2024.03.010

Doan, L., Pham, N. V., Nguyen, P. B., Le, Q. N., Phung, T. K. and Ngo, T. T., Marine algae as sustainable platforms for the green synthesis of metal nanoparticles, *ACS Omega*, 11(10), 15598–15616 (2026). https://doi.org/10.1021/acsomega.5c12334

El-Belely, E. F., Farag, M. M., Said, H. A., Amin, A. S., Azab, E., Gobouri, A. A. and Fouda, A., Green synthesis of zinc oxide nanoparticles (ZnO-NPs) using Arthrospira platensis (Class: Cyanophyceae) and evaluation of their biomedical activities, *Nanomater.*, 11(1), 95 (2021). https://doi.org/10.3390/nano11010095

Ezealisiji, K. M., Siwe-Noundou, X., Maduelosi, B., Nwachukwu, N. and Krause, R. W., Green synthesis of zinc oxide nanoparticles using *Solanum torvum* (L.) leaf extract and evaluation of the toxicological profile of the ZnO nanoparticles-hydrogel composite in Wistar albino rats, *Int. Nano Lett.*, 9(2), 99–107 (2019). https://doi.org/10.1007/s40089-018-0263-1

Fouda, A., Saied, E., Eid, A. M., Kouadri, F., Alemam, A. M., Hamza, M. F., Alharbi, M., Elkelish, A. and Hassan, S. E. D., Green synthesis of zinc oxide nanoparticles using an aqueous extract of *Punica granatum* for antimicrobial and catalytic activity, *J. Funct. Biomater.*, 14(4), 205 (2023). https://doi.org/10.3390/jfb14040205

Gunasekaran, R., Jyotsnika, K., Kannan, K. and Sivaperumal, P., Unlocking the bioactive potential: ZnO NPs synthesized from Chaetomorpha linum aqueous extract, *Next Nanotechnol.*, 9, 100346 (2026). https://doi.org/10.1016/j.nxnano.2025.100346

Hamad, R. S., Elshaer, M. A. A., El-Mahdy, H. A., Mohammed, O. A., Jeelani, M., Doghish, A. S., Abd-Elraheem, M. A. M., Abdel mageed, M. M., Darwish, A. A. E., Ibrahim, E. K. and El-Dakroury, W. A., Green-synthesized zinc oxide nanoparticles using Echinops spinosus extract: A promising anticancer agent for hepatocellular carcinoma, *Plos one*, 20(10), e0331171 (2025). https://doi.org/10.1371/journal.pone.0331171

Ifeanyichukwu, U. L., Fayemi, O. E. and Ateba, C. N., Green synthesis of zinc oxide nanoparticles from pomegranate (*Punica granatum*) extracts and characterization of their antibacterial activity, *Mol.*, 25(19), 4521 (2020). https://doi.org/10.3390/molecules25194521

Ishwarya, R., Vaseeharan, B., Kalyani, S., Banumathi, B., Govindarajan, M., Alharbi, N. S., Kadaikunnan, S., Al-Anbr, M. N., Khaled, J. M. and Benelli, G., Facile green synthesis of zinc oxide nanoparticles using Ulva lactuca seaweed extract and evaluation of their photocatalytic, antibiofilm and insecticidal activity, *J. Photochem. Photobio. B: Bio.*, 178, 249-258 (2018). https://doi.org/10.1016/j.jphotobiol.2017.11.006

Islam, K. S., Mustak, M. H., Shishir, M. K. H., Karim, M. M. and Khan, G. M. A., Biosynthesis of ZnO nanoparticles using banana peel pectin for antibacterial and photocatalytic applications, *South African J. Chem. Eng.*, 52(1), 127-140 (2025). https://doi.org/10.1016/j.sajce.2025.02.002

Kalaba, M. H., El-Sherbiny, G. M., Ewais, E. A., Darwesh, O. M. and Moghannem, S. A., Green synthesis of zinc oxide nanoparticles (ZnO-NPs) by *Streptomyces baarnensis* and its active metabolite (Ka): a promising combination against multidrug-resistant ESKAPE pathogens and cytotoxicity, *BMC Microbiol.*, 24(1), 254 (2024). https://doi.org/10.1186/s12866-024-03392-4

Kiwumulo, H. F., Muwonge, H., Ibingira, C., Lubwama, M., Kirabira, J. B. and Ssekitoleko, R. T., Green synthesis and characterization of iron oxide nanoparticles using *Moringa oleifera*: a potential protocol for use in low- and middle-income countries, *BMC Res. Notes*, 15(1), 149 (2022). https://doi.org/10.1186/s13104-022-06039-7

Marica, I., Nekvapil, F., Ștefan, M., Farcău, C. and Falamaș, A., Zinc oxide nanostructures for fluorescence and Raman signal enhancement: a review, *Beilstein J. Nanotechnol.*, 13(1), 472–490 (2022). https://doi.org/10.3762/bjnano.13.40

Mirza, A. U., Kareem, A., Nami, S. A., Khan, M. S., Rehman, S., Bhat, S. A., Mohammad, A. and Nishat, N., Biogenic synthesis of iron oxide nanoparticles using *Grewia optiva* and *Prunus persica* phytospecies: characterization, antibacterial and antioxidant activity, *J. Photochem. Photobiol. B*, 185, 262–274 (2018). https://doi.org/10.1016/j.jphotobiol.2018.06.009

Mohammadian, M., Es'haghi, Z. and Hooshmand, S., Green and chemical synthesis of zinc oxide nanoparticles and size evaluation by UV-visible spectroscopy, *J. Nanomed. Res.*, 7(1), 00175 (2018). http://dx.doi.org/10.15406/jnmr.2018.07.00175

Mongy, Y. and Shalaby, T., Green synthesis of zinc oxide nanoparticles using Rhus coriaria extract and their anticancer activity against triple-negative breast cancer cells, *Scientific Reports,* 14(1), 13470 (2024). https://doi.org/10.1038/s41598-024-63258-7

Muhammad, W., Ullah, N., Haroon, M. and Abbasi, B. H., Optical, morphological and biological analysis of zinc oxide nanoparticles (ZnO NPs) using *Papaver somniferum* L., *RSC Adv.*, 9(51), 29541–29548 (2019). https://doi.org/10.1039/c9ra04424h

Palanisamy, S., Rajasekar, P., Vijayaprasath, G., Ravi, G., Manikandan, R. and Prabhu, N. M., A green route to synthesize silver nanoparticles using *Sargassum polycystum* and its antioxidant and cytotoxic effects: an *in vitro* analysis, *Mater. Lett.*, 189, 196–200 (2017). https://doi.org/10.1016/j.matlet.2016.12.005

Pillai, A. M., Sivasankarapillai, V. S., Rahdar, A., Joseph, J., Sadeghfar, F., Rajesh, K. and Kyzas, G. Z., Green synthesis and characterization of zinc oxide nanoparticles with antibacterial and antifungal activity, *J. Mol. Struct.*, 1211, 128107 (2020). https://doi.org/10.1016/j.molstruc.2020.128107

Rahman, M. A., Vishala, D., Hasnain, S. M., Paramasivam, P. and Ayanie, A. G., Review of gold nanoparticles: synthesis, properties and applications, *Discover Metals*, 59(1), 4 (2026). https://doi.org/10.1007/s13404-026-00370-8

Rajeshkumar, S., Kumar, S. V., Ramaiah, A., Agarwal, H., Lakshmi, T. and Roopan, S. M., Biosynthesis of zinc oxide nanoparticles using *Mangifera indica* leaves and evaluation of their antioxidant and cytotoxic properties in lung cancer (A549) cells, *Enzyme Microb. Technol.*, 117, 91–95 (2018). https://doi.org/10.1016/j.enzmictec.2018.06.009

Rizvi, M., Gupta, R., Kumar, S. and Banerjee, M., Biogenic, facile, and sustainable pathway of obtaining ZnO-PS nanoparticles through Pisum sativum waste peels, their characterization and cytotoxic assessment against HeLa cell line via experimental and computational methods, *Next Nanotechnol.*, 9, 100322 (2026). https://doi.org/10.1016/j.nxnano.2025.100322

Sahith, V. N., Kumar, A., Lakshmi, D., Renukadevi, M., Sruthi, V. S. and Revathi, S., Green fabrication of zero-valent iron nanoparticles (nZVI) from *Senna auriculata* flower extract for antidiabetic activity, *J. Environ. Nanotechnol.*, 15(2), 344–353 (2026). https://doi.org/10.13074/jent.2026.26.2622254

Shobier, A. H., Hassan, S. W. and Ghani, S. A. A., Seaweed-derived bioactives: a promising source of novel therapeutics, *Blue Economy*, 4(1), 4 (2026). https://doi.org/10.57241/2805-2994.1051

Sivaranjani, V. and Parthiban, P., Antioxidant, Antimicrobial, and Potential Biomedical Applications of Green Synthesized Silver Nanoparticles Using Aloe barbadensis Root, *J. Environ. Nanotechnol.*, 14(1), 97-104(2025). https://doi.org/10.13074/jent.2025.03.2511226

Sugimoto, R., Lee, L., Tanaka, Y., Morita, Y., Hijioka, M., Hisano, T. and Furukawa, M., Zinc Deficiency as a General Feature of Cancer: a Review of the Literature, *Bio. Trace Ele. Res.*, 202(5), 1937-1947 (2024). https://doi.org/10.1007/s12011-023-03818-6

Umar, H., Kavaz, D. and Rizaner, N., Biosynthesis of zinc oxide nanoparticles using *Albizia lebbeck* stem bark and evaluation of its antimicrobial, antioxidant and cytotoxic activities on human breast cancer cell lines, *Int. J. Nanomed.*, 14, 87–100 (2019). https://doi.org/10.2147/IJN.S186888

Vijayakumar, N., Bhuvaneshwari, V. K., Ayyadurai, G. K., Jayaprakash, R., Gopinath, K., Nicoletti, M., Alarifi, S. and Govindarajan, M., Green synthesis of zinc oxide nanoparticles using *Anoectochilus elatus*, and their biomedical applications, *Saudi J. Bio. Sci.*, 29(4), 2270-2279 (2022). https://doi.org/10.1016/j.sjbs.2021.11.065

Yusefi, M., Shameli, K., Ali, R. R., Pang, S. W. and Teow, S. Y., Evaluating anticancer activity of plant-mediated synthesized iron oxide nanoparticles using *Punica granatum* fruit peel extract, *J. Mol. Struct.*, 1204, 127539 (2020). https://doi.org/10.1016/j.molstruc.2019.127539

Zangeneh, A., Zangeneh, M. M. and Moradi, R., Ethnomedicinal plant extract-assisted green synthesis of iron nanoparticles using *Allium saralicum* extract and their antioxidant, cytotoxicity, antibacterial, antifungal and cutaneous wound-healing activities, *Appl. Organomet. Chem.*, 34(1), e5247 (2020). https://doi.org/10.1002/aoc.5247